

Extremely Low $V_{\pi} \times L$ Slow Light Photonic Crystal Modulator with GHz Bandwidth

Xiaochuan Xu^{1*}, Amir Hosseini^{2*}, Harish Subbaraman^{2*}, Che-Yun Lin¹, Somayeh Rahimi¹, and Ray T. Chen¹

1. Microelectronics Research Center, The University of Texas at Austin, Austin, TX 78758, USA
2. Omega Optics, Inc., 10306 Sausalito Dr, Austin, TX 78759, USA
xiaochuan.xu@mail.utexas.edu

Abstract—We demonstrated a GHz bandwidth slow light photonic crystal waveguide based PIN Mach-Zehnder modulator with $V_{\pi} \times L$ as low as 0.0464 V·mm, which is the lowest figure of merit reported so far.

Keywords—slow light; photonic crystal; Mach-Zehnder modulator

I. INTRODUCTION

Slow light in photonic crystal waveguides (PCWs) has been extensively studied for potential on-chip applications such as optical buffers and enhanced non-linearity due to increased light-matter interaction [1, 2]. The enhanced light-matter interaction provided by the slow light operation can be exploited, resulting in ultra-compact on-chip photonic devices [3]. Over 40GHz modulation speed using the slow light mode in slot photonic crystals refilled with electro-optic (EO) polymer has been demonstrated [4]. High-yield and repeatable low-dispersion slow-light devices can be achieved by fabrication-friendly dispersion engineering of PCWs [5]. We have recently shown that due to the existence of the evanescent modes at the boundary between two photonic crystals with different group indices, short (8-16 periods) step-couplers can be used for efficient coupling between single mode silicon strip waveguides and slow light PCWs [6].

These advances render PCWs as reliable solutions for improvement of microwave/RF photonic devices and systems. Increasing the slope-efficiency is a broad bandwidth way of increasing the optical link gain, which in turn reduces the Noise Figure [7]. Reducing the switching voltage of the modulator, V_{π} , in order to enhance the slope-efficiency of the modulator is the most effective technique for reducing 1) the noise of the optical source AKA Relative Intensity Noise, RIN, 2) resistive thermal noise at the receiving end, and 3) the shot noise of the optical detector [8]. It is also crucial to reduce the optical modulator length (L) to minimize the RF and optical signals velocity mismatch and well as the RF loss that limit the bandwidth of operation. Overly, the optical modulator to be used in the microwave photonic based sensor must have the smallest possible $V_{\pi} \times L$. In this paper we report a Mach Zehnder Interferometer (MZI) modulator based on low-

dispersion slow-light PCWs with the lowest $V_{\pi} \times L$ reported to the best of our knowledge.

II. DESIGN AND SIMULATION

A schematic of the band engineered PCW is shown in Fig. 1(a). The lattice constant $a=392\text{nm}$. The thickness of the silicon layer and the buried oxide layers are 250nm and 3 μm , respectively. Group indices of the top cladding, core layer, and the bottom cladding materials are $n_{\text{air}}=1$, $n_{\text{si}}=3.47$, $n_{\text{siO}_2}=1.45$, respectively. Dispersion engineering is done by shifting the 3 innermost rows parallel to the defect line [5] with the parameters s_1 , s_2 , and s_3 as depicted in Fig. 1(a). Figure 2(b) shows the band diagram for the dispersion engineered PCW with $dW=0$, $s_1=0$, $s_2=-0.05a$, $s_3=0.25a$, and $r=0.27a$, where dW is the change in the width of the defect line with respect to a W1 PCW, and r is the hole radius.

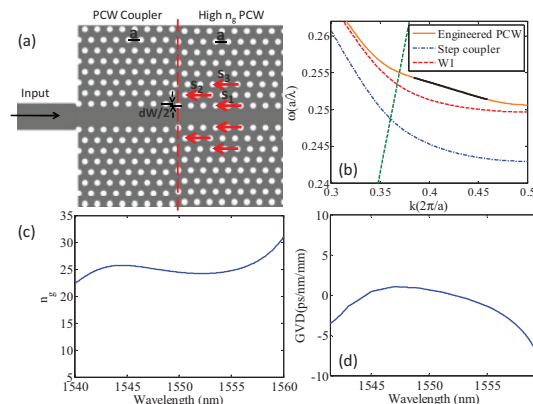


Figure.1 (a) a schematic of band engineered PCW and PCW taper. (b) Band structures of the designed band-engineered PCW and step PCW coupler. The low-dispersion slow-light bandwidth is highlighted by a black line on the defect mode of the designed band-engineered PCW. Silica light line ($n=1.45$) is shown by a dashed green light. (c) Variations of the group index and (d) group index dispersion over the bandwidth of interest.

Variations of the group index and group index dispersion as functions of the wavelengths are shown in Figures 2(c) and (d), respectively. In order to efficiently couple the PCW with input and output strip silicon waveguides, an 8-period long step coupler is designed,

This work is sponsored by Air Force Office of Scientific Research (AFOSR) Small Business Innovative Research (Grant No. FA 9550-11-C-0014) monitored by Dr. Gernot Pomrenke

$dW=0.15a$, $s_1=0$, $s_2=0$, $s_3=0$, and $r=0.27a$. The band diagram of the PCW coupler is depicted in Fig. 1(b) that shows an overlap between the low-dispersion slow-light bandwidth of the engineered PCW and the low-dispersion fast-light bandwidth of the PCW coupler. A symmetric MZI is designed by placing two $98\mu\text{m}$ long PCWs at the two arms. 1×2 Multimode Mode Interference couplers (MMIs) are used for beam splitting/combining as shown in Fig. 2(a). One of the PCWs is doped to form a PIN as shown in Fig. 2(b). The length of the electrodes along the PCW is $80\mu\text{m}$.

III. FABRICATION AND TESTING

The modulator was fabricated on a Unibond silicon-on-insulator wafer with a 250 nm top silicon layer and $3\mu\text{m}$ buried oxide layer. Photonic crystal waveguides, photonic crystal tapers and strip waveguides are patterned in one step with a JEOL JBX-6000FS electron-beam lithography system followed by reactive ion etching. The windows for P^+ and N^+ implantation were opened by photolithography. Ion implantations of Boron at 30 KeV and phosphorus at 50 KeV were performed to obtain an average doping concentration about $5\times 10^{19}\text{ cm}^{-3}$. The thermal rapid annealing for 1 min at 950°C in a flowing nitrogen environment was performed afterwards to anneal the lattice defects and activate the implanted ions. Electrode contact windows were then opened by photolithography and the native oxide inside the windows was removed. Aluminum electrodes were made by electron-beam evaporation and a subsequent lift off process. Finally, a good ohmic contact was formed by post metallization annealing at a temperature of 400°C for 30 mins [3].

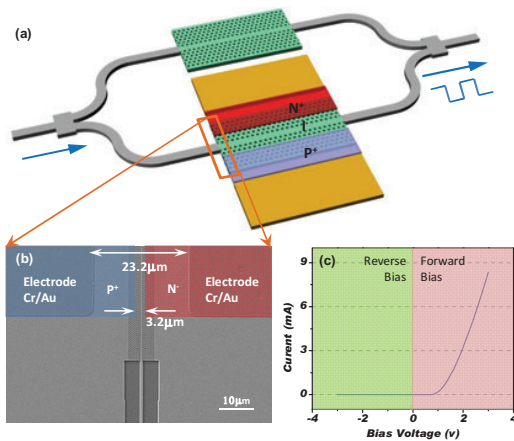


Figure.2 (a) schematic of photonic crystal MZI modulator; (b) scanning electronic microscope image of the active arm of the modulator; (c) static characteristic of the PIN diode.

The static characteristic of the PIN diode obtained with Agilent B1500a semiconductor parameter analyzer is shown in Fig. 1(c). The forward linear resistance is $\sim 200\text{ Ohm}$. Measurements of the figure of merit $V_\pi\times L$

and data transmission, described below, were carried out by coupling light from a TE-polarized tunable laser into the device through butt coupling and tuning wavelength to 1550.48 nm . The modulated output was detected with a gain switchable photodetector. The voltage V_π required to produce a carrier injection-induced π phase shift was measured by applying a 100 kHz triangular electrical drive signal, as shown in Fig. 3(a), to a MZI modulator under a forward bias $V_{\text{bias}} = 1.25\text{ V}$. The drive amplitude was increased until the slope of the modulated optical signal changed sign at the peaks/troughs of the drive waveform, as illustrated in Fig.3(a) [9]. A complete half-period of optical modulation was observed for a peak-to-peak applied voltage of $V_\pi = 0.58\text{ V}$, leading to a figure of merit of $V_\pi\times L = 0.0464\text{ V}\cdot\text{mm}$, which is less than one third of the lowest $V_\pi\times L$ reported so far [9]. Figure 3(b) shows the 2GHz optical waveform.

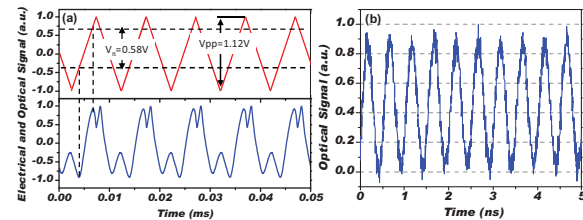


Figure.3 (a) triangular electrical drive signal with a V_{pp} of 1.12V and V_{offset} of 1.25V (top). The over modulated optical signal indication a V_π of 0.58V (bottom) ; (b) the optical signal of 2GHz operation.

IV. CONCLUSION

In this paper, we presented a slow light photonic crystal based MZI modulator with $V_\pi\times L$ as low as $0.0464\text{ V}\cdot\text{mm}$, which is the lowest value reported so far. 2GHz operation of this modulator is also demonstrated

*The authors contribute to the paper equally.

REFERENCES

- [1] R. W. Boyd, D. J. Gauthier, and A. L. Gaeta, *Optics & Photonics News*, vol. 17, no. 4, pp. 18-23, 2006.
- [2] Y. A. Vlasov, M. O'Boyle, H. F. Hamann, and S. J. McNab, *Nature*, vol. 438, pp. 65-69, 2005.
- [3] L. Gu, W. Jiang, X. Chen, and R. T. Chen, *IEEE J. Sel. Top. Quantum Electron.*, vol. 14, no. 4, pp. 1132-1139, 2008.
- [4] J. H. Wülbern, S. Prorok, J. Hampe, A. Petrov, M. Eich, J. Luo, A. K.-Y. Jen, M. Jenett, and A. Jacob, *Opt. Lett.*, vol. 35, no. 16, pp. 2753-2755, 2010.
- [5] S. Rahimi, A. Hosseini, X. Xu, H. Subbaraman, and R. T. Chen, *Opt. Express*, vol. 19, no. 22, pp. 21832-21841, 2011.
- [6] A. Hosseini, X. Xu, H. Subbaraman, D. Kwong, W. Jiang, and R. T. Chen, *Appl. Phys. Lett.*, vol. 98, no. 3, pp. 031107 - 031107, 2011.
- [7] C. H. Cox III, E. I. Ackerman, G. E. Betts, and J. L. Prince, *IEEE Trans. Microwave Theory Tech.* vol. 54, no. 2, pp. 906-920, 2006.
- [8] S. Iezekiel, John Wiley & Sons, Ltd., Chichester – UK, 20
- [9] H. C. Nguyen, Y. Sakai, M. Shinkawa, N. Ishikura, and T. Baba, *Opt. Express*, vol. 19, no. 14, pp. 13000-13007, 2011